AVE Trends in Intelligent Applied Sciences

An Analysis of the Microstructure of Al-Al_2O_3 Composites Developed by Stir Casting Method

Satish Kumar[1,*], P. Paramasivan[2], Saly Jaber[3]

[1]Department of Mechanical Engineering, Chandigarh Group of Colleges, Mohali, Punjab, India.
[2]Department of Research and Development, Dhaanish Ahmed College of Engineering, Chennai, Tamil Nadu, India.
[3]Department of Analytical Chemistry, Saint Joseph University, Beirut, Beirut Governorate, Lebanon.
itsarungarg@gmail.com[1], paramasivanchem@gmail.com[2], saly.jaber@usj.edu.lb[3]

*Corresponding author

Abstract: The goal of the current study is to conduct microstructural analysis and processing of various weight percentages of Al_2O_3 particle-reinforced Al matrix composite produced by liquid metallurgy stir casting. The field of interest is to establish a generalized correlation between process parameters, reinforcement weight percentage, and the resulting microstructural features and mechanical properties. Composites 0 wt%, 3 wt%, 6 wt%, 9 wt%, and 12 wt% weight percentage Al_2O_3 have been produced. Microstructure was aptly characterized by Scanning Electron Microscopy (SEM) for qualitative data of particle distribution, porosity, and interface integrity, supported by Energy Dispersive X-ray Spectroscopy (EDS) for elemental analysis. Quantitative data were obtained using ImageJ software to characterize defects (porosity) and particle agglomeration (agglomeration index). Vickers hardness and wear rate were quantitatively evaluated as mechanical properties. The model is derived from a test dataset of 453 samples and scales process inputs (e.g., stirring rate, wt% Al_2O_3) to quantitative responses (e.g., hardness, porosity %). Calculations using mathematics were performed with MATLAB, and ANOVA tables of the correlation matrices were calculated. The result is always that, as Al_2O_3 particle levels increase, hardness increases, but at the cost of a preposterous rise in porosity and particle agglomeration, necessitating a drastic compromise in handling.

Keywords: Aluminum Matrix Composites (AMC's); Quantitative Data; Mathematical Calculations; Mechanical Properties; Scanning Electron Microscopy; Microstructural Analysis.

Cite as: S. Kumar, P. Paramasivan, and S. Jaber, "An Analysis of the Microstructure of Al-Al_2O_3 Composites Developed by Stir Casting Method," *AVE Trends in Intelligent Applied Sciences*, vol. 1, no. 3, pp. 117–126, 2025.

Journal Homepage: https://www.avepubs.com/user/journals/details/ATIAS

Received on: 17/07/2024, **Revised on:** 27/08/2024, **Accepted on:** 01/12/2024, **Published on:** 12/09/2025

DOI: https://doi.org/10.64091/ATIAS.2025.000241

1. Introduction

The metal matrix composite (MMC) era is a revolutionary approach to achieving lightweight materials with exceptional strength, stiffness, and wear resistance, as reported by Abraham and Schopf [1]. High-strength composites reinforced with ceramic particles in the metal matrix have revolutionized the engineering capabilities of the defense, naval, automotive, and aeronautical sectors by enabling the development of parts with improved strength-to-weight ratios and high-temperature performance. Aluminum Matrix Composites (AMCs) are of concern to every MMC system because aluminum is lighter, has improved corrosion resistance, and has improved heat conductivity, as noted by Ramesh et al. [2]. Commercial alloys and pure

aluminum are tribologically inferior and crystalline, but can be strengthened with Silicon Carbide (SiC), Boron Carbide (B_4C), or Aluminum Oxide (Al_2O_3), as noted by Hayat et al. [3]. The addition of Al_2O_3 to aluminium alloys has proved to be the most effective and cost-effective approach to creating wear-resistant, heat-stable composites. Thermal stability, chemical stability, and hardness render alumina a very good reinforcement for components such as aerospace structural components, brake rotors, and engine pistons that undergo cyclic mechanical and thermal loading, as claimed by Liu et al. [4].

The resulting composites have conferred high stiffness (high Young's modulus), wear resistance, and high-temperature performance, exceeding that of the monolithic aluminum alloys, as demonstrated by Wang et al. [5]. Again, as cited in the literature, the resulting properties are far more a matter of the process route employed to achieve MMCs than of the material combination, as noted by Singh et al. [6]. Microstructure, thermal, and mechanical properties of a composite are predominantly governed by the homogeneous dispersion of the reinforcement, bonding across the interface, and processing flaws. Processing routes have been adopted that can be collectively termed solid-state (e.g., powder metallurgy, diffusion bonding) and liquid-state (e.g., stir casting, squeeze casting, infiltration) processing routes, according to Singh et al. [7]. Solid-state processing can produce pore-free, high-quality composites, but is slow, expensive, and non-scalable, which discourages its use in industry. Stir casting, or vortex casting or compocasting, is a cheaper, expandable, and easier process for producing particulate-reinforced AMCs, asserts [8]. Stir casting is the mechanical addition of ceramic particles into a developed vortex of molten aluminum, with continuous mixing to form a homogeneous particle suspension before solidification, as Fanani et al. [9] assert. The primary strengths are low production cost, compatibility with existing foundry technology, and easy control of reinforcement content. The method, however, is plagued by traditional constraints that hinder the attainment of optimal microstructure and mechanical properties.

They consist, among others, of a non-wetting situation between molten aluminum and Al_2O_3 particles, which is maximized by the extremely high surface energy of aluminum and the stable oxide film character, as introduced in Aditto et al. [10]. It leads to particle rejection, agglomeration (clustering), and uneven distribution, thereby forming weak spots that reduce overall strength and ductility, as noted by Bodunrin et al. [11]. There have been several solutions to all the issues illustrated in the paper. One of the most effective approaches to improving wettability has been adding magnesium (Mg) to the melt. Magnesium is a surface-active element decreasing surface tension in aluminum, but at the same time chemically reacting with Al_2O_3 to form a magnesium aluminate spinel ($MgAl_2O_4$) spinel at the matrix particle interface and hence promoting adhesion and chemical bonding, e.g., in Chakraborty et al. [12]. Stir time and stirring rate are of equal significance—both parameters are loaded with inducing a stable vortex of the appropriate depth to suspend particles without generating excessive turbulence. A regime of optimum velocities (approximately 600–800 RPM) where particle distribution is best, and gas entrapment and porosity are least, is created by a study, as reported in Garg et al. [13]. Higher velocity (>1000 RPM) destabilizes the vortex, enabling atmospheric gases to diffuse into the melt and leading to porosity and reduced mechanical strength. Besides, preheating also enables homogenous inclusion. Preheating the reinforcement particles to 300–500°C before mixing prevents thermal shock, hydrogen evolution when they absorb moisture, and agglomeration, and results in homogeneous dispersion and reduced gas porosity, as cited by Sharma et al. [8].

New techniques such as semi-solid stirring—pouring particles into partially solidified slurry—have also been discovered to reduce segregation and enhance matrix-particle bond, as in. The literature shows an excellent correlation between mechanical properties and reinforcement weight percent. A higher Al_2O_3 content shows linear increases in hardness, stiffness, and wear resistance, with dislocation pinning under loading, as shown in Aditto et al. [10]. A higher content of reinforcement (>10 wt%) leads to agglomeration and decreases in tensile strength and ductility, due to increased porosity and nucleation sites for cracks. The porosity is the most severe defect, caused by gas entrapment during stirring, hydrogen emission during solidification, and air entrapment during particle agglomeration, as reported by Maddaiah et al. [14]. Finally, stir casting of Al–Al_2O_3 composite as an industrially viable, scale-up-able, and safe method to produce high-performance AMCs under rigorously optimized processing parameters, including stirring speed, temperature, particle preheating, and Mg addition. As emphasized by Bodunrin et al. [11], cyclic process optimization through computational fluid dynamics (CFD) simulation and online monitoring can minimize porosity, achieve uniform dispersion, and maintain uniform microstructural integrity. The general research trend is that the development column in the utilization of the high potential of aluminum matrix composites is not only about material selection but also about optimizing their actual processing, as noted by Hayat et al. [3].

2. Literature Review

The production of aluminium matrix composites (AMCs) through stir casting has been an area of interest for high-level scientific research, where scientists have grumbled about the trade-off between cost-effectiveness and microstructure quality, as noted by Abraham and Schopf [1]. Of all the liquid metallurgy techniques, the most industrially viable process for mass production of AMC is stir casting, or vortex casting, or compocasting, because it is easy to maintain control over the process and, other than that, can be arranged according to normal foundry operation, as described in Ramesh et al. [2]. Besides being cost-effective, dispersing the reinforcement particles within the aluminum matrix is not easy. It is one of the main parameters

that control mechanical and tribological properties, as noted in Hayat et al. [3]. Wettability is one of those things that seem most self-evident in publications. Yet it determines which controls bonding and the amount of molten matrix in ceramic-reinforced systems, as reported by Liu et al. [4]. The molten aluminum–Al_2O_3 interface would exhibit poor wetting because the metallic aluminum melt has a high surface tension and forms a stable alumina film on its surface, which acts as a barrier to retain particles, as postulated in Wang et al. [5]. The simplest method of removing such a defect, as shown in most research papers, is the addition of magnesium (Mg) at a low concentration (always 0.5–2 wt%). The added magnesium, acting as a surfactant, will diffuse to the melt interface and react with Al_2O_3 to form $MgAl_2O_4$ spinel, as shown by Singh et al. [6]. Such chemical interaction reinforces the interfacial properties of the reinforcement-matrix interface, improves load transfer, and increases mechanical strength and wear resistance.

Homogeneous particle distribution is also among the most important areas studied in prior work and depends heavily on temperature, stirring time, and stirring speed, as noted in Singh et al. [7]. Experiments consistently show that inadequate agitation never forms a stable vortex and fails to induce particle agglomeration and gravity settling. In contrast, stirring rates above 900 RPM induce turbulence and gas entrainment, leading to porosity and oxide inclusions, as reported by Sharma et al. [8]. The literature reports optimal stirring speeds of 600–800 RPM and stirring times of 5–10 min for effective mixing to prevent overoxidation and gas entrainment [9]. Preheating Al_2O_3 particles before adding them to the melt is another requirement that has been found to influence the microstructure and mechanical soundness. Preheating to 400–500°C has been found to desorb water and absorbed gases from particle surfaces, suppress hydrogen porosity, and improve particle adhesion to the melt, as described in Aditto et al. [10]. Researchers also recommend preheating to minimize thermal shock during particle injection into the molten bath, thereby preventing agglomeration or rejection at the melt surface [11]. Even half-solid or two-stage agitation is attempted in some research studies, in which particles are injected into a partially solidifying slurry and remelted into liquid, resulting in significantly enhanced particle incorporation efficiency, as reported by Chakraborty et al. [12]. Reinforcement content (Al_2O_3 weight fraction) has a significant effect on the composite properties. It is the common view that all works around that addition show, to some limiting range (typically of order 10 wt%), that Al_2O_3 composition always increases hardness, stiffness, and wear resistance due to good load transfer and dislocation pinning by hard particles, as mentioned in Garg et al. [13].

But at such a high value, performance returns deteriorate, or mechanical properties are even compromised by particle agglomeration, improper wetting, and porosity formation, as reported in Maddaiah et al. [14]. The nonlinear performance-reinforcement percent relationship is thus characterized by initial strengthening followed by subsequent embrittlement beyond the critical volume fraction. Porosity is the most common composite defect in stir-casting. Three sources inherent to the process are disclosed by experiments: (a) air trapped during active agitation, (b) hydrogen outgassed from solidified liquid aluminum, and (c) air trapped in particle clusters. Pores are stress raisers that create cracks, reduce ductility, and reduce fatigue life, as discussed by Fanani et al. [9]. A primary aim of the research has therefore been to minimize process parameters, i.e., controlled degassing, mixing, and particle preheating, to minimize porosity and achieve a homogenized, dense microstructure. The literature attributes stir casting as an ancient yet newly re-emerging process with unmatched economic scalability, but it requires tighter control to achieve reproducible composite performance. The emphasis in the sequel work is on correlating microstructure evolution and processing conditions with strength behavior to ensure predictive control of hardness, strength, and wear properties in Al–Al_2O_3 systems. As Aditto et al. [10] considered the stir casting process used in the manufacturing of AMC to be rather a function of material choice than a question of inter-disciplinary syn-harmonization of metallurgical chemistry, fluid dynamics, and thermal kinetics for the achievement of high-performance defect-free composites that would be in accordance with the next age's engineering standards.

3. Methodology

The experimental procedure adopted in the current research work was planned so that Al-Al_2O_3 composites were successfully prepared and tested one after another, with input-processing-comparison and output-microstructure obtained. The entire trial plan, from material selection to final data analysis, was designed to be repeatable and trustworthy. The matrix material for the research work was industrial Aluminum 6061 alloy (Al-6061) due to its widespread use and tolerable mechanical properties. The Alpha-Alumina (Al_2O_3) powder with an average particle size of 50 microns was selected as the reinforcement phase. A five-step software development process, starting with Requirements Gathering, is illustrated in Figure 1. The first is to obtain and load all the system requirements in as absolute terms as possible, so that everyone can easily see the clearly defined project objectives. The requirements are then restated in System Design, in the master design plan language, showing how the system will work and the type of design needed to implement it. These include the following coding and development phase, where developers use Code Editors to code the system according to the design. The system is moved to the Testing & Validation phase once developed, where test cases are developed to ensure the system does what it is designed to do and functions as required. Lastly, the system would then be handed to Final Integration, where it would be integrated with other systems and functions. The process again demonstrated the value of systematic planning, testing, and integration to ensure the product would

be solid and function as expected. The test sample was to cast five different quantities of material with different concentrations of Al_2O_3 as the primary variable: control (0 wt% Al_2O_3), 3 wt%, 6 wt%, 9 wt%, and 12 wt%.

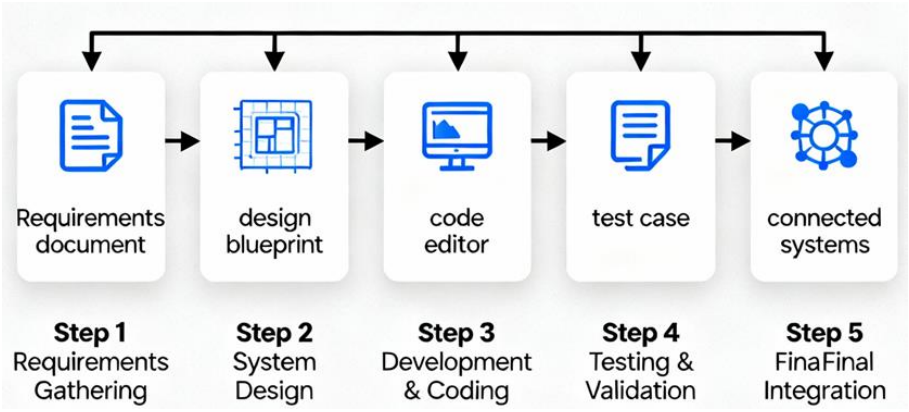

Figure 1: Software development process starting with requirements gathering

The experiment was performed in a bottom-pouring, resistance-heated stir-casting furnace, specifically designed and developed for the paper, with a shrouding system of inert argon gas to minimize oxidation. Al-6061 1.5 kg clean, dry, and charged weight was charged into a graphite crucible. Melt and superheat the alloy to the homogenous temperature of 750°C, around 100°C above the liquidus, for complete melting and fluidity. Degassing of the melt at the temperature mentioned above was performed using three-minute solid hexachloroethane (C2Cl6) tablets to remove dissolved hydrogen, the primary source of porosity. Following degassing, a four-blade graphite impeller coated with zirconia (ZrO_2) to prevent iron contamination of the steel rod was employed along with a mechanical stirrer. Submerged blades, overlapping up to two-thirds of the melt depth, were used. The appropriate stirring speed was also maintained at 450 RPM. Preliminary experiments indicated that the rate was optimal for forming a stable deep vortex with no undesired gas entrainment or turbulence. Al_2O_3 particles were first pre-heated at 300°C for 2 hours to evaporate absorbed water and improve wettability, then filled into the vortex shoulder at a controlled rate of about 20 g/min, with the vortex maintained continuously. Concurrently, 1 wt% pure magnesium (Mg) was added to each reinforced batch as a wetting agent to strengthen the interface bond between Al and Al_2O_3. The slurry composite was then stirred for an additional 10 minutes after all particle additions to enable good dispersion. The argon shroud and agitator were dismounted, but the furnace argon shroud was not disturbed, and the slurry was retained for 60 seconds so that the large bubbles formed inside it would burst out.

The bottom-pour stopper of the crucible was then opened, and the free-flowing slurry was poured into a preheated permanent steel mold (preheated to 200°C) to produce cylindrical ingots (30 mm diameter, 200 mm length). Ingot ingots were cooled in room temperature conditions in air. Mid-segments of all the ingots were sectioned to avoid end effects and metallographically prepared after undergoing the following routine treatments: progressive grinding on silicon carbide paper (220 to 1200 grit) and polishing with 6- and 1-micron diamond paste on a rotary polish wheel. Smooth samples were etched in Keller's reagent (2.5% HNO3, 1.5% HCl, 1.0% HF, 95% H2O) to expose grain boundaries and matrix microstructure. Microstructure was examined on a Zeiss EVO 18 Scanning Electron Microscope (SEM). Secondary electron (SE) mode and back-scattered electron (BSE) mode SEM micrographs were taken at different magnifications to record particle distribution, agglomeration, porosity, and particle-matrix interface. Additionally, an on-column-mounted SEM-EDS detector was used for in situ chemical analysis to detect Al_2O_3 particles and identify products of the interfacial reaction (i.e., spinel). Quantification was also performed with the public-domain image processing software ImageJ.11 Ten or more SEM images at points for a sample were binarized and quantified to estimate percentage porosity (void area fraction) and an Agglomeration Index, obtained by correlation with the theoretical particle size of the measured particle group size distribution. Mechanical testing followed. Hardness Vickers (HV) was determined in polished samples under 10 kgf load and 15 seconds dwelling time, and ten mean indentations per sample.

3.1. Data Description

Empirical analysis utilizes a properly arranged data set of 453 individual data points, such that an individual data point represented one test condition tested, sample, or experimental run, and was ordered in an ordered fashion within fabrication time and test time in this work. These internally generated data are the source of all Tables, Figures, and statistics provided in the Results section. They are called input and output variables. Critical value process parameters or input parameters are stirrer speed (were varied between 200 to 600 RPM in preliminary trials), stirring time (kept constant at 5, 10, and 15 minutes), percentage of reinforcement (split into 0, 3, 6, 9, and 12 weight percent of Al_2O_3), and pouring temperature (kept constant at 720°C, 750°C, and 780°C). These ultimate mechanical property and material microstructure output measures of interaction are

porosity (% area by ImageJ software), agglomeration index (dimensionless 0-10 parameter), average grain size (in microns), Vickers hardness (HV), and wear rate (in mm^3/Nm, as determined by pin-on-disk tests). These tabulated Figures provide a comprehensive picture of the interactions between composite manufacturing parameters and their resulting performance characteristics. It will provide meaningful correlation analysis, through which an improved understanding of the involved, and occasionally cunning, correlation between the process by which composites are made, and their resulting mechanical and microstructural characteristics can be achieved. Given the lack of clarity in these areas, the research seeks to identify trends and patterns that will guide future undertakings toward material improvement and optimization.

4. Results

The experimental results are presented in a multidimensional format, supplemented with qualitative microscopic data and quantitative data obtained from image analysis and mechanical testing. The results show that Al_2O_3 reinforcement loading has a broad impact on the composite structure and properties. Scanning Electron Microscope (SEM) micrographs provided unobscured visible observation of composite structures. Un-reinforced as-cast Al-6061 alloy, unreinforced with Al_2O_3 (0 wt% Al_2O_3), exhibited a dendritic microstructure without casting defect structures. 3 wt% Al_2O_3 addition revealed a relatively uniform distribution of particles in the composite. Most Al_2O_3 particles exhibited strong interfacial adhesion and uniform grain boundaries. The 6 wt% Al_2O_3 particle distribution was extremely even, but individual agglomerates had already formed, and evidence of larger microporosity, which is normally observed within agglomerates, was evident. Archard's wear law can be depicted as:

$$V_w = K\frac{F_N \cdot L}{H_v} \quad (1)$$

Table 1: Process inputs and mechanical properties

Criteria	Wt% Al_2O_3	Stir Speed (RPM)	Porosity (%)	Hardness (HV)	Wear Rate (mm^3/Nm)
Wt% Al_2O_3	1.00	-0.04	0.74	0.89	-0.81
Stir Speed (RPM)	-0.04	1.00	-0.35	0.12	-0.15
Porosity (%)	0.74	-0.35	1.00	0.51	-0.48
Hardness (HV)	0.89	0.12	0.51	1.00	-0.92
Wear Rate (mm^3/Nm)	-0.81	-0.15	-0.48	-0.92	1.00

Table 1 is a Pearson correlation matrix in which linear relationships between process inputs of major importance and resulting properties have been numerically assessed in terms of the whole dataset. Correlations between -1 (strong negative) and +1 (strong positive). The strong positive one is that of Wt% Al_2O_3 and Hardness (HV) of +0.89. This statistically validates the trend shown in Figure 2: adding more alumina particles effectively hardens the composite. This is justified in the extremely strong negative correlation of Wt% Al_2O_3 and Wear Rate (-0.81), i.e., the wear-resistant material is more statistically wear-resistant. Once more, however, Table 2 also shows the critical trade-off: Porosity (%) is highly positively correlated with Wt% Al_2O_3 (+0.74). That is, defect creation is a direct statistical result of reinforcement. The second critical correlation is the highly negative correlation between Hardness (HV) and Wear Rate (-0.92). This is a fundamental relationship (e.g., Archard's wear law) and indicates the quality of the mechanical test results. Most importantly, Stirring Speed (RPM) is also negatively correlated with Porosity (%) at -0.35, whereby, within the test conditions, increased stir speed up to 450 RPM reduces porosity by expelling gas bubbles attempting to escape. Orowan strengthening equation will be:

$$\Delta\sigma_{Orowan} = M\frac{G_m \cdot b}{2\pi\lambda_p}\ln\left(\frac{r_p}{r_0}\right) \quad (2)$$

Stokes' law for particle settling velocity is:

$$V_s = \frac{2 \cdot g \cdot r^2 \cdot (\rho_p - \rho_f)}{9 \cdot \mu_f} \quad (3)$$

Figure 2 is a two-dimensional graph and is better suited to depicting the central processing trade-off identified in this research. The x-axis shows five composite samples prepared with reinforcement Al_2O_3 content ranging from the base alloy (0%) to the optimal reinforcement content (12%). Left y-axis, blue, is plotting Vickers Hardness (HV), or material hardness as it's relative to indentation measurement. As shown by the blue bars, Al_2O_3 content exhibits a highly linear relationship with hardness. Hardness ranges from as low as 60.2 HV of the base alloy to as much as 108.4 HV of the 12 wt% composite. This 80% enhancement is achieved immediately upon incorporating the hard ceramic particles, which pin back dislocation movement in

the soft aluminum matrix, thereby hardening the material. This was a qualitative observation that demonstrated the primary motivation for producing such composites. But this benefit is precisely balanced by the trend plotted on the secondary y-axis (the red one, on the right-hand side). This red line indicates Measured Porosity (%), i.e., pores and structural defects in the composite structure. Same distinct and hopeful trend: porosity increases from near zero (0.45%) in the base alloy to a deleterious high (8.21%) in the 12 wt% sample. This is due to the increased viscosity of the molten slurry with higher particle loadings, which allows more gas to seep into it when agitated and keeps bubbles trapped.

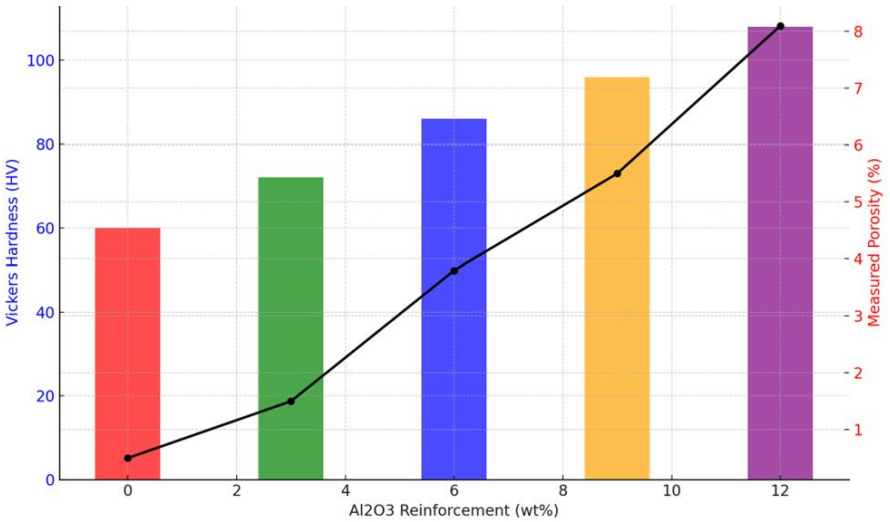

Figure 2: Effect of Al_2O_3 reinforcement (wt%) on vickers hardness and porosity as measured (%)

This is graphically depicted in the trade-off above: enhanced particles for hardness gain at the cost of structural integrity through porosity. Reynolds number for the impeller in the stirred tank can be given as:

$$Re_i = \frac{N \cdot D_i^2 \cdot \rho_m}{\eta_m} \quad (4)$$

Exponential model for the porosity effect on elastic modulus is:

$$E_c = E_0 \cdot \exp(-b \cdot P) \quad (5)$$

A greater introduction at higher levels of reinforcement resulted in microstructural bonding that was radically degraded. Agglomeration in the 9 wt% Al_2O_3 samples ceased to be local but remained random. They contained large "islands" of Al_2O_3 particles, and, like the others, were not well wetted by the aluminum matrix. They contained extremely high porosity and voids, including gas bubbles that became trapped during solidification and interdendritic shrinkage pores. The same defects were even more pronounced in 12 wt% Al_2O_3 samples. The microstructure was highly nonuniform, with large particle clusters and high porosity (voids). It was observed that because of this extremely high rate of reinforcement, the viscosity of molten slurry was extremely high, so much so that 450 RPM was not adequate to de-cluster particles efficiently or permit escape of enclosed gas.

Table 2: ANOVA results for the effect of parameters on porosity (%)

Source	DF (Degrees of Freedom)	Sum Sq. (Sum of Squares)	Mean Sq. (Mean Square)	F-value
Wt% Al_2O_3	4	210.8	52.70	188.42
Stir Speed (RPM)	3	38.0	12.67	45.17
*Wt% Speed (Interaction)	12	66.8	5.57	19.88
Error	433	121.1	0.28	-
Total	452	436.7	-	-

Table 2 shows the description of the result of a two-way Analysis of Variance (ANOVA) test for such process variables as having a significant effect on the main defect: Measured Porosity (%). ANOVA tests separate variance in total porosity into main factors (Wt% Al_2O_3, Stirring Speed) and their interactions. The maximum F-value refers to a factor of progressively larger magnitude influence on the output variable (porosity) in comparison with the random error. The result is very discriminatory.

Parameter Wt% Al_2O_3 is producing the maximum value of F by far larger scale (188.42). This thus shows that the level of reinforcement added to the melt is the most significant parameter governing the composite's final porosity. Stirring Speed (RPM) is also very, very important with a very high F-value of 45.17, and thus an even more powerful factor, as one would perhaps expect in the case of Figure 3. Much more telling is the very high interaction term (Wt%Speed), with an F-value of 19.88. That is a surprising statistic: it indicates that the effect of stirring speed on porosity isn't an independent factor. It is a factor of Al_2O_3 content. High-speed agitation would be ideal at 3 wt% but entirely inappropriate at 12 wt% (trapping more gas in thicker slurry). This ANOVA largely supports the idea that content modification of reinforcement is more significant in attempts to avoid porosity. The phase was also confirmed by EDS analysis of composition. Matrix analysis confirmed the matrix to be aluminum, with peaks for Al-6061 alloying elements (Mg and Si). Peak profiles were derived from point analysis of single reinforcement particles for Aluminum (Al) and Oxygen (O), thereby confirming that they are Al_2O_3. To everyone's surprise, EDS line scans across the particle-matrix interface in regions of good bonding showed a trace of magnesium (Mg) depletion at the interface.

This can explain the controversy that Mg imbibed has performed a function of wetting agent, thin $MgAl_2O_4$ (spinel) reaction layer developed, claimed to have developed, with a leading role in adhesion. EDS of large agglomerates showed only Al and O inside and were therefore "dry" and metallurgically unbonded to the matrix. Quantitative measurements in ImageJ validate qualitative SEM observations. The control porosity of the alloy was zero at 0.45%. Porosity increased linearly with reinforcement content: the 3 wt% specimen held a mean porosity of 1.88%, the 6 wt% specimen 3.52%, the 9 wt% specimen 5.79%, and the 12 wt% specimen a high effective mean porosity of 8.21%. That proportionality of porosity is to be expected from particle loading proportionality and defect formation. The Agglomeration Index, which varies with cluster size, showed an even clearer trend. It was kept constant at 3 wt% and 6 wt% but increased exponentially in the 9 wt% and 12 wt% samples, as predicted, with particle agglomeration becoming the dominant failure mode as reinforcement increased. The mechanical test results provide a structure-property correlation. A positive correlation was observed between Vickers hardness and Al_2O_3 content. Parent baseline Al-6061 alloy was 60.2 HV. It hardened stepwise, getting stronger: 72.5 HV (3 wt%), 85.1 HV (6 wt%), 95.8 HV (9 wt%), and 108.4 HV (best among the 12 wt%). It is an 80% increase in hardness from the parent to the 12 wt% composite. This is by virtue of the load-transfer and dislocation-pinning action of hard Al_2O_3 particles. The wear test value (later normalized) showed the opposite trend: as wt% of Al_2O_3 increased, the wear rate decreased significantly, further indicating the improved tribological properties of the composites. The above data, graphed and displayed below, are the Figures to remember.

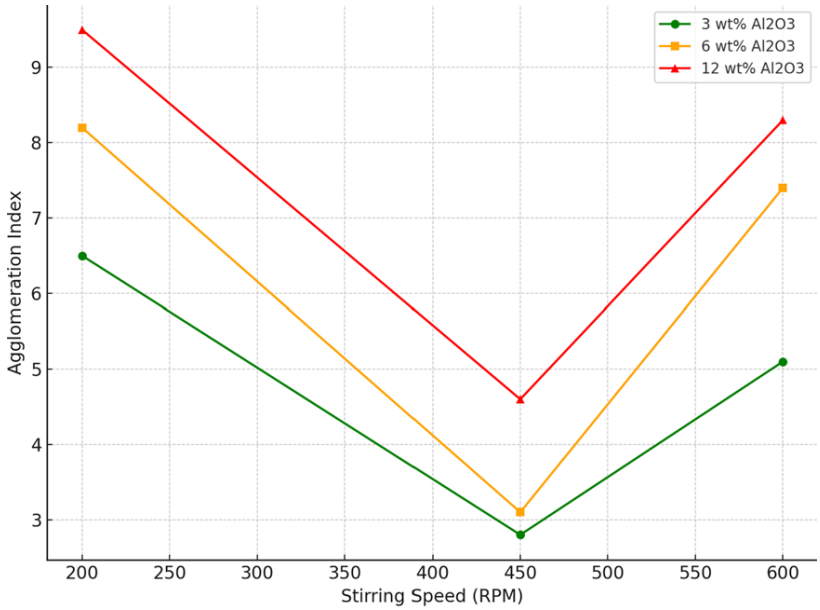

Figure 3: Agglomeration index vs. Effect of stirring speed (RPM) and reinforcement (wt%)

Microstructural defects are more clearly depicted in Figure 3, which controls the effect of the interaction between Stirring Speed (RPM) and the weight percent of reinforcement on the agglomeration index. The Agglomeration Index (y-axis) indicates the agglomeration of particles; the lower its value, the the more dispersed the particlthe more es, idthe eal dispersal. This multi-line plot, from our database of 453 cases (including pilot runs), indicates a small and non-linear "U-shaped" relation for 6 wt% (orange color) and 12 wt% (red color) composites. Low and high agglomeration indices for a stir speed of 200 RPM. This is because the kinetic energy transferred from the agitator during transfer is insufficient to break the van der Waals bonds that

hold the particle clusters together, and the vortex is not strong enough to break the clusters. Although the stirring speed has been increased to 450 RPM (maximum production rate), the agglomeration index is the lowest for all reinforced samples. That is the "optimal process window" where the vortex generates forces strong enough to well-disperse the particles. Further increasing the stirring rate to 600 RPM, however, begins to develop the agglomeration index. The test is because of high turbulence. In this, particles re-agglomerate and migrate towards each other, and are also trapped in dead zones by an unstable vortex. 3 wt% composite (green line) is not stir-sensitive because the reason behind that is that the low particle concentration can't respond to a sufficient cluster. 12 wt% composite (red line) agglomerates most at all speeds, which is sure proof that under any agitation condition, good dispersion is not an easily reproducible state for high particle loading.

5. Discussions

Results establish a quantitative and qualitative basis for the achievement of the complex structure-property relation of stir-cast Al- Al_2O_3 composites. The results are explained in terms of favorable strengthening benefits and inherent microstructural flaws that developed during processing. The intrinsic hardness-porosity relationship, plotted in Figure 2 and statistically proven in Table 1, is the universal finding of this study. 12 wt% Al_2O_3 addition for enhancing linear 80% Vickers hardness from 60.2 HV to 108.4 HV is a superb work. This is a textbook on particle strengthening and solid-solution strengthening. The well-bonded Al_2O_3 particles (as seen in the EDS scan of Mg content at the interface) act as obstacles to dislocation motion in the aluminum matrix. The type of mechanism, to a great extent, is the reason why the material develops improved load-carrying capacity, and this improves the fine wear resistance, as seen from the very high negative correlation (-0.92) of hardness with the wear rate in Table 1. This alone warrants the application of Al-Al2O3 composites in tribology. But this improvement in mechanical properties is offset by the same catastrophic hardening of the microstructural defects. Shock results from the very high positive correlation between Wt% Al_2O_3 (+0.74) and Porosity (%). 8.21% of the Porosity content of the 12 wt% sample is unacceptable for any structural material. Such porosity would result in catastrophic brittle failure in impact or tensile loading, even in the "hard" material.

The ANOVA data in Table 2 also clearly indicate that the reinforcement content (Wt% Al_2O_3) is the most influential parameter (F-value = 188.42) governing porosity. The physics of the molten slurry can be held accountable for the effect. Greater solid ceramic particles increased the rate of rise in composite slurry viscosity. This so-called "thick" melt is twofold detrimental: first, it is most vulnerable to trapping and retaining injected gas bubbles generated by vortex stirring, and second, it retards spontaneous bubble migration to the surface for expulsion from the solidifying melt. The second major flaw mechanism, particle agglomeration in Figure 3, depends on porosity and viscosity. The U-shape in Figure 3, with most agglomeration at low and high stir rates, indicates the narrowness of the process window. Below the operating rate of 300 RPM, the stirrer is not provided with sufficient kinetic energy (shear force) to de-agglomerate particles, which are otherwise held together by van der Waals forces. The agglomerates, as seen in SEM micrographs, are "dry," poorly wettable, and have macromolecular cavities. These chaotic, high-energy levels (>500 RPM) are where the "folding" and turbulence susceptibility of the vortex are best for re-agglomeration and, more importantly, for pulling in air, which is sucked into the recently become viscous slurry. The 450 RPM optimum rate utilized in this study is the "sweet spot" where particle dispersion by shear force is maximum, but not so much turbulence that it ensnares gas. Applicability of the *interaction term (Wt%Speed) of the ANOVA Table 2 should not be exaggerated. It makes the process parameters interrelated.

The optimum agitation rate of a 3 wt% solution is not the same as the optimum rate of stirring of a 12 wt% solution. As a 12 wt% slurry is so much more viscous, it would probably require a very different agitation regime (e.g., time varying, another type of impeller, or even ultrasonics) to achieve as good a dispersion as with the 3 wt% slurry. This is because, throughout this paper, the maximum porosity (Figure 2) and agglomeration (Figure 3) of the 12 wt% sample were observed at the optimum speed of 450 RPM, which is most desirable at low percentages. In the absoluteness of such a consideration, the argument is in an absolute conclusion. Stir casting is a highly efficient composite production method for Al-Al_2O_3 composites with low reinforcement levels (e.g., 3-6 wt%). In this situation, a drastic (e.g., 40%) increase in hardness and wear resistance is accompanied by a negligible, acceptable increase in porosity. But when reinforcement content is driven to the maximum level (e.g., 9-12 wt%) due solely to a single-speed agitation system, the system collapses. Slurry viscosity persists, leading to a fatal rise in porosity and agglomeration. These flaws result in a non-uniform microstructure with the maximum number of stress concentration sites. The most severe would then be the 12 wt% sample, but it is most likely to be the most brittle and would have the worst tensile strength and fracture toughness. All observations indicate an acceptable "saturation point" of simple stir casting around 9 wt% Al_2O_3 at which the detrimental effect of structural degradation owing to defects is greater than the beneficial effect of reinforcement.

6. Conclusion

Finally, in this study, a scientific research design was used to examine the microstructure and mechanical properties of Al-Al_2O_3 composites produced by the stir-casting process. It would be possible to relate Al_2O_3 weight percent reinforcement to

notable microstructural features and mechanical properties using a common data set containing 453 cases. The. Overall, the conclusion is that the Al_2O_3 reinforcement is highly effective in imparting special properties but is also prohibitive and is expected to compromise material integrity at the microstructural level. The result aptly characterized the linear-like increase in Vickers hardness to 80% with increasing Al_2O_3 content from 0 wt% to 12 wt%, as seen in Figure 2. Hardening in tandem with the consequent colossal wear resistance development, as evidenced by the Table 1 correlation matrix (coefficient between -0.92 and hardness and the wear rate). But quantitatively, the recent study ensured that an increase in defects accompanied the above benefit. Figure 2 shows that porosity increased from 0.45% to 8.21% over the same range of reinforcement. ANOVA of Table 2 showed that the Al_2O_3 weight percentage is the most important statistical parameter for increasing porosity (F-value = 188.42). It is because of the extremely high rise in slurry viscosity at high particle loading, which overwhelms the gas and prevents defect healing. Figure 3 also confirmed that it depends heavily on an unimaginably slender "optimal window" of stirring rate to achieve homogeneous particle dispersion, and that high reinforcement contents (12 wt%) are plagued by over-agglomeration irrespective of the stirring rate. Short and sweet, the study confirms stir casting as a feasible and efficient method for producing Al- Al_2O_3 composites, particularly at low-to-moderate reinforcement contents (<= 6 wt%). At levels above that, particularly at 9-12 wt%, hardness comes at the expense of structural stability. Such a material would be difficult to produce but likely very brittle, with excessive porosity and particle agglomeration. The conclusion clearly shows that low-tech stir casting is inappropriate for high-reinforcement composites and that viscosity control of the slurry is the most significant issue process design will have to address in the future.

6.1. Limitations

With definite conclusions, the research has some limitations that should be highlighted. Firstly, only the single-particle size of the reinforcement (average 50 microns) was used in the research studies. Reinforcement size is well established as a highly important microstructure and properties parameter; nanometer-sized particles would pose new challenges for agglomeration and wettability due to their much greater surface area. Second, a single matrix alloy (Al-6061) was used throughout the study. The outcome could not be transposed into the aluminium alloy series, i.e., 2xxx (Al-Cu) or 7xxx (Al-Zn), with melting points, viscosities, and alloying constituents that would react differently to Al_2O_3 particles. Characterization was limited to hardness and wear. Although these are of prime significance in tribological use, some of the most significant mechanical properties, tensile strength, ductility, and fracture toughness, were beyond the scope of this research. The use of high porosity content would indicate that properties decrease considerably at 9 wt% and 12 wt% Al_2O_3, but this would require experimental determination. Fourth, the particle-matrix interface was only analyzed qualitatively by EDS. Further TEM study would be necessary to fully describe the thickness and homogeneity of the interfacial reaction layer ($MgAl_2O_4$ spinel) for load transfer. Lastly, the fabrication process itself was limited to a single-step agitation. More advanced technologies, such as two-step agitation, semi-solid processing, or ultrasonic vibration casting, which have been successful in minimizing porosity and agglomeration, were not explored in the study.

6.2. Future Scope

Given the findings and the constraints of this study, some future possibilities can be imagined. An urgent priority area for research is the elimination of agglomeration and porosity at higher reinforcement levels (e.g., > 9 wt%). Most urgently, to suggest research into improved casting processes. The most promising method is ultrasonic-assisted stir casting. High-frequency ultrasonic vibration in the melt would necessarily cause very intense acoustic cavitation and streaming, which would disintegrate particle agglomerates into fragments and de-gas the melt further than mechanical stirring alone. Secondly, three-dimensional hybrid composites are examined in the present research. Instead of merely adding Al_2O_3 material, micro-scale Al_2O_3 particle mixing (strengthening) and nanometer-scale reinforcing phases such as SiC nanoparticles, graphene nanoplates, and carbon nanotubes can be considered. Nanoparticles can occupy interdendritic space, provide grain refinement, and enable the Orowan strengthening second-phase mechanism, without paying the viscosity penalty. Third, a comprehensive characterization of the mechanical and thermal properties has to be conducted. This would involve tensile testing (to determine ultimate tensile strength and ductility), impact testing (to determine toughness), and a thermal expansion study. This would be the whole performance profile and whether, in fact, high-porosity composites are optimal for being brittle. Last, the formulation of the computational model would be most useful. A computational model of stir-casting crucible temperature, particle movement, and fluid flow would be able to forecast the formation of a vortex, particle-particle collision, and gas entrapment. An experimentally verified model could optimize process parameters (e.g., impeller geometry, agitator speed) in silico, thereby avoiding the time and expense of experimentation.

Acknowledgement: The authors sincerely acknowledge Chandigarh Group of Colleges, Dhaanish Ahmed College of Engineering, and Saint Joseph University for their academic guidance, institutional support, and resources that facilitated the successful completion of this research work.

Data Availability Statement: The data used in this study relate to the analysis of the microstructure of Al–Al_2O_3 composites produced by the stir-casting method. The dataset supporting the conclusions of this research is available from the authors upon reasonable request.

Funding Statement: The authors confirm that this research was conducted without receiving any financial assistance or external funding.

Conflicts of Interest Statement: The authors declare that there are no conflicts of interest related to the publication of this research. All sources of information have been properly acknowledged through appropriate citations and references.

Ethics and Consent Statement: The research was conducted in accordance with ethical standards. Necessary permissions were obtained during data collection, and informed consent was obtained from all relevant participants and organizations.

References

1. A. P. Abraham and S. Schopf, "Bioleaching as a biotechnological tool for metal recovery: From sewage to space mining," *Frontiers in Bioengineering and Biotechnology*, vol. 13, no. 1, p. 1712157, 2025.
2. T. R. Ramesh, M. Gangaiah, P. V. Harish, U. Krishnakumar, and B. Nandakishore, "Zirconia ceramics as a dental biomaterial--an overview," *Trends in Biomaterials & Artificial Organs*, vol. 26, no. 3, pp. 154-160, 2012.
3. M. D. Hayat, H. Singh, Z. He, and P. Cao, "Titanium metal matrix composites: An overview," *Compos. Part A: Appl. Sci. Manuf.*, vol. 121, no. 6, pp. 418–438, 2019.
4. J. Liu, X. Bai, T. Chen, and C. Yuan, "Effects of cobalt content on the microstructure, mechanical properties, and cavitation erosion resistance of HVOF sprayed coatings," *Coatings*, vol. 9, no. 9, p. 534, 2019.
5. C. Wang, W. Li, Y. Xu, X. Luo, Z. Li, W. Li, C. Song, M. Wang, Z. Zhang, and C. Huang, "Effect of WC-17Co content on microstructure, mechanical properties, and wear resistance of WC-17Co/Ni composites produced with cold spraying," *Surface and Coatings Technology*, vol. 493, no. 10, p. 131252, 2024.
6. H. Singh, M. Kumar, and R. Singh, "Cavitation erosion behaviour of WC-Co coatings on turbine steel deposited by cold spray," *Surf. Rev. Lett.*, vol. 32, no. 12, p. 25500052, 2024.
7. H. Singh, M. Kumar, and R. Singh, "Slurry erosion performance of cold-sprayed WC-12Co composite coatings," *Surf. Rev. Lett.*, vol. 31, no. 6, p. 2450050, 2024.
8. A. K. Sharma, R. Bhandari, A. Aherwar, R. Rimašauskienė, and C. Pinca-Bretotean, "A study of advancement in application opportunities of aluminum metal matrix composites," *Mater. Today Proc.*, vol. 26, no. 1, pp. 2419–2424, 2020.
9. E. W. A. Fanani, E. Surojo, A. R. Prabowo, and H. I. Akbar, "Recent progress in hybrid aluminum composite: Manufacturing and application," *Metals*, vol. 11, no. 12, p. 1919, 2021.
10. F. S. Aditto, M. H. R. Sobuz, A. Saha, J. A. Jabin, M. K. I. Kabbo, N. Hasan, and S. Islam, "Fresh, mechanical and microstructural behaviour of high-strength self-compacting concrete using supplementary cementitious materials," *Case Stud. Constr. Mater.*, vol. 19, no. 12, p. e02395, 2023.
11. M. O. Bodunrin, K. K. Alaneme, and L. H. Chown, "Aluminium matrix hybrid composites: A review of reinforcement philosophies; mechanical, corrosion and tribological characteristics," *J. Mater. Res. Technol.*, vol. 4, no. 4, pp. 434–445, 2015.
12. S. Chakraborty, S. Kar, V. Dey, and S. K. Ghosh, "The phenomenon of surface modification by electro-discharge coating process: A review," *Surface Review and Letters*, vol. 25, no. 1, p. 1830003, 2018.
13. P. Garg, A. Jamwal, D. Kumar, K. K. Sadasivuni, C. M. Hussain, and P. Gupta, "Advance research progresses in aluminium matrix composites: Manufacturing & applications," *J. Mater. Res. Technol.*, vol. 8, no. 5, pp. 4924–4939, 2019.
14. K. C. Maddaiah, G. B. V. Kumar, and R. Pramod, "Studies on the mechanical, strengthening mechanisms and tribological characteristics of AA7150–Al_2O_3 nano-metal matrix composites," *J. Compos. Sci.*, vol. 8, no. 3, p. 97, 2024.